International Journal of Mass Spectrometry 309 (2012) 49–55

Contents lists available at SciVerse ScienceDirect

International Journal of Mass Spectrometry

journal homepage: www.elsevier.com/locate/ijms

Structures of $Al^+(C_2H_4)_n$ clusters: Mass-selected photodissociation and *ab initio* calculations

Jinyun Yuan, Yuchao Zhao, Gaolei Hou, Zhen Gao, Weijun Zheng *

Beijing National Laboratory for Molecular Sciences, State Key Laboratory of Molecular Reaction Dynamics, Institute of Chemistry, Chinese Academy of Sciences, Beijing 100190, China

ARTICLE INFO

Article history:
Received 23 May 2011
Received in revised form 26 August 2011
Accepted 26 August 2011
Available online 3 September 2011

Keywords:
Mass spectrometry
Mass-selection
Photodissociation
Aluminum-ethene

ABSTRACT

$Al^+(C_2H_4)_n$ clusters were produced by reaction of laser ablated Al^+ ions with ethene molecules seeded in a pulsed molecular beam, and detected with a reflectron time-of-flight mass spectrometer. The mass spectrum shows that an Al^+ ion can combine with at least eight ethene molecules to form $Al^+(C_2H_4)_n$ clusters. Based on the photodissociation experiments and *ab initio* calculations, we suggest that an Al^+ ion can strongly interact with one or two C atoms to form Al–C σ-bonds and trigger addition reaction of ethene molecules to develop chain or ring structures. The interaction of Al^+ ion with ethene is different from the interaction between V^+ ion and ethene molecules reported previously (Int. J. Mass. Spectrom. 295 (2010) 36), wherein a V^+ ion can only combine with no more than four ethene molecules at similar experimental conditions and causes little change in the structures of the ethene molecules.

1. Introduction

Investigations of metal ion-hydrocarbon molecular interactions have received extensive interests because such interactions play important roles in various chemical fields, such as catalysis, lubrication, hydrogen storage, oxidation and reduction reactions [1–3]. In catalysis processes, bond-formation and bond-breaking usually occur at unsaturated metal centers. Electron-deficient aluminum complexes are important for the study of homogeneous and heterogeneous catalysis [4,5], for example, the zeolites doped by Al have been widely used as heterogeneous catalysts due to its high activity, good selectivity and chemical stability [6–8]. Since aluminum and its compounds are important in heterogeneous catalysts, the interaction between aluminum ion and organic molecules received special attention. Kasai and McLeod examined the electron spin resonance (ESR) spectra of aluminum–ethene complex in rare-gas (neon and argon) matrices. They found that the $Al(C_2H_4)$ complex had a π-coordinated structure with a dative bond of donation from a half-full p orbital of Al into the antibonding π orbital of ethene [9,10]. Mitchell et al. determined the binding energy between Al atom and ethene to be greater than 0.69 eV by observation of the temperature dependence of the equilibrium constant of the Al–ethene reaction in the range of 288–333 K [11]. Manceron and Andrews investigated the infrared spectrum of $Al(C_2H_4)$ in solid argon and ethene. They showed that Al atom formed a symmetric π-complex with ethene by interacting with equivalent CH_2 groups [12]. Chenier et al. [13] detected the formation of alumiocyclopentane in the reaction of Al atom with ethene molecules at low temperature by ESR method. Schwarz and co-workers determined the structure and bond dissociation energy of Al–ethene using FTICR mass spectroscopy and *ab initio* calculations [14]. Kleiber and co-workers studied photodissociation spectroscopy of $Mg^+(C_2H_4)$ and $Al^+(C_2H_4)$ [1,15]. They also reported photodissociation spectroscopy studies of weakly bound Al^+–alkene bimolecular complexes (ethene, propene, and 1-butene) in the 216–320 nm range [16]. The geometric structure and electronic property of $Al(C_2H_4)$ were also investigated using different theoretical methods by several theoreticians [17–20].

In the past, the investigations of aluminum with ethene molecules were mainly focused on Al–C_2H_4 complex with a single ethene molecule except that $Al(C_2H_4)_2$ was studied by Chenier et al. [13]. To our knowledge, there is no investigation on the cationic $Al^+(C_2H_4)_{2-6}$ clusters. In this work, we studied the interaction between Al^+ ion and ethene molecules using mass-selected photodissociation of $Al^+(C_2H_4)_n$ clusters combining with *ab initio* calculations.

2. Experimental and computational methods

2.1. Experimental method

The experiments were conducted on a home-built reflectron time-of-flight mass spectrometer, which has been described in detail elsewhere [21]. Aluminum–ethene clusters were generated in a laser vaporization source, where a rotating and translating aluminum disc target was ablated by the second harmonic of a Nd:YAG

* Corresponding author. Tel.: +86 10 62635054; fax: +86 10 62563167.
E-mail address: zhengwj@iccas.ac.cn (W. Zheng).

1387-3806/$ – see front matter © 2011 Elsevier B.V. All rights reserved.
doi:10.1016/j.ijms.2011.08.026

laser (532 nm, 2.331 eV/pulse, Continuum Surelite II-10) to produce Al^+ ions, then the Al^+ ions reacted with the ethene molecules seeded in argon carrier gas (~4% ethene) expanding into the laser vaporization source through a pulsed valve (General Valve Series 9) at 3–5 atm backing pressure. The formed aluminum–ethene clusters were then mass-analyzed with the reflectron time-of-flight mass spectrometer. The $Al^+(C_2H_4)_n$ (n = 1–6) cluster ions were each mass-selected, decelerated and then photodissociated with a second Nd:YAG laser at 1064, 532, 355 and 266 nm wavelengths, respectively. The fragment and parent ions were detected by the MCP (microchannel plate) detector of the mass spectrometer. The ion signals were amplified with a broadband amplifier and recorded with a 100 MHz digital oscilloscope card, then collected in a laboratory computer with a home-made software.

2.2. Computational method

The theoretical calculations of $Al^+(C_2H_4)_n$ (n = 1–3) clusters were performed with MP2 method [22] and using 6-311+G(d,p) basis sets implemented in the Gaussian03 software package [23]. The vibrational frequency calculations were performed at the optimized geometric structures of each isomer and transition state. It has been confirmed that all isomers have no imaginary frequencies, and each transition state has the unique imaginary frequency. The internal reaction coordinate (IRC) calculations were performed to ensure that each transition state indeed corresponds to the two expected isomers. The zero-point vibrational energy corrections and basis set superposition error were considered for all the energies. The calculations were performed for the temperature of 298 K.

3. Results and discussion

3.1. Experimental

3.1.1. Mass spectrum

A typical mass spectrum of $Al^+(C_2H_4)_n$ clusters is presented in Fig. 1. The prominent mass peaks are $Al^+(C_2H_4)_n$ (n = 0–8) clusters. The mass signals of $Al^+(C_2H_4)_9$ and $Al^+(C_2H_4)_{10}$ clusters can also be detected although they are not shown in the spectrum. From Fig. 1, we can see that the ion intensities decrease gradually from $Al^+(C_2H_4)$ to $Al^+(C_2H_4)_3$, then increase from $Al^+(C_2H_4)_3$ to $Al^+(C_2H_4)_4$, after that the ion intensities decrease from $Al^+(C_2H_4)_4$ to $Al^+(C_2H_4)_8$ again. In addition to the $Al^+(C_2H_4)_n$ series, the low intensity mass peaks of $Al^+(H_2O)(C_2H_4)_n$ (n = 0–8) clusters were also detected due to the existence of trace amounts of water molecules in the carrier gas.

3.1.2. Photodissociation mass spectra

To explore the structures and relative stabilities of these clusters, each of the $Al^+(C_2H_4)_n$ (n = 1–6) clusters was mass-selected and photodissociated using 1064, 532, 355 and 266 nm photons. We detected different fragment ions from the dissociations of $Al^+(C_2H_4)_n$ (n = 1–6) clusters at 266 nm wavelength. Fig. 2 depicts the photodissociation mass spectra of $Al^+(C_2H_4)_n$ (n = 1–6) at 266 nm wavelength. At 355 nm, we detected the fragment ions from the dissociation of $Al^+(C_2H_4)_2$ and $Al^+(C_2H_4)_3$ clusters only, no fragment ion was detected for $Al^+(C_2H_4)$ and $Al^+(C_2H_4)_{4-6}$. The dissociation mass spectra of $Al^+(C_2H_4)_2$ and $Al^+(C_2H_4)_3$ clusters at 355 nm wavelength are similar to those at 266 nm. Therefore, they are not shown here (see the Supplementary data). At 1064 and 532 nm wavelengths, no fragment ion was detected for any of the $Al^+(C_2H_4)_n$ (n = 1–6) clusters.

As shown in Fig. 2, for the dissociation of $Al^+(C_2H_4)$, the Al^+ fragment ion is produced through elimination of one neutral ethene molecule. The Al^+ ion is the only fragment ion from the dissociation of $Al^+(C_2H_4)_2$, indicating two ethene molecules are eliminated together.

Dissociation of $Al^+(C_2H_4)_3$ produces $Al^+(C_2H_4)$ and Al^+ fragment ions. It is possible that the $Al^+(C_2H_4)$ fragment ion is generated via loss of two neutral ethene molecules from parent ion $Al^+(C_2H_4)_3$ since no $Al^+(C_2H_4)_2$ fragment ion appears. It is possible that the Al^+ fragment ion is mainly produced directly from parent ion $Al^+(C_2H_4)_3$ by eliminating three ethene molecules instead of from the secondary dissociation of the $Al^+(C_2H_4)$ fragment ion since the dissociation efficiency of $Al^+(C_2H_4)$ fragment ion is very low.

$Al^+(C_2H_4)_2$, $Al^+(C_2H_4)$ and Al^+ fragment ions were detected from dissociation of parent $Al^+(C_2H_4)_4$ cluster. Among them, the $Al^+(C_2H_4)_2$ is generated via loss of two ethene molecules from the parent $Al^+(C_2H_4)_4$ cluster. $Al^+(C_2H_4)$ fragment ion is probably produced through the loss of three ethene molecules from the parent $Al^+(C_2H_4)_4$ cluster, rather than from the secondary dissociation of $Al^+(C_2H_4)_2$ since dissociation of parent $Al^+(C_2H_4)_2$ cluster does not produce $Al^+(C_2H_4)$ fragment ion as shown in the previous paragraph. The Al^+ fragment ion is mainly from the loss of four ethene molecules from parent $Al^+(C_2H_4)_4$ cluster or from the secondary dissociation of $Al^+(C_2H_4)_2$ or $Al^+(C_2H_4)$ fragment ions.

Regarding the photodissociation of $Al^+(C_2H_4)_5$ cluster, $Al^+(C_2H_4)_3$, $Al^+(C_2H_4)_2$, $Al^+(C_2H_4)$ and Al^+ fragment ions were detected. The $Al^+(C_2H_4)_3$ fragment ion is generated through loss of two ethene molecules from parent $Al^+(C_2H_4)_5$ cluster. The $Al^+(C_2H_4)_2$ fragment ion is probably produced through eliminating three ethene molecules from parent $Al^+(C_2H_4)_5$ rather than from the secondary dissociation of $Al^+(C_2H_4)_3$ fragment since dissociation of $Al^+(C_2H_4)_3$ can not produce $Al^+(C_2H_4)_2$ fragment ion. It is likely that the $Al^+(C_2H_4)$ is generated from parent $Al^+(C_2H_4)_5$ or the secondary dissociation of $Al^+(C_2H_4)_3$. Similarly, Al^+ is generated through dissociation of parent $Al^+(C_2H_4)_5$ or the secondary dissociation from $Al^+(C_2H_4)_3$, $Al^+(C_2H_4)_2$ or $Al^+(C_2H_4)$ fragment ions.

For the dissociation of $Al^+(C_2H_4)_6$ at 266 nm, four fragments ions, $Al^+(C_2H_4)_3$, $Al^+(C_2H_4)_2$, $Al^+(C_2H_4)$ and Al^+ were observed. The $Al^+(C_2H_4)_3$ fragment ion is produced through loss of three ethene molecules from parent $Al^+(C_2H_4)_6$. Since photodissociation of $Al^+(C_2H_4)_3$ can not produce $Al^+(C_2H_4)_2$ fragment ion, the $Al^+(C_2H_4)_2$ fragment ion here is probably generated via loss of four ethene molecules from parent $Al^+(C_2H_4)_6$. The $Al^+(C_2H_4)$ fragment ion may be generated via loss of five ethene molecules from the parent $Al^+(C_2H_4)_6$ or the secondary dissociation of the $Al^+(C_2H_4)_3$. And the Al^+ fragment ion is from dissociation of parent $Al^+(C_2H_4)_6$ or the secondary dissociation of the fragment $Al^+(C_2H_4)_3$, $Al^+(C_2H_4)_2$ or $Al^+(C_2H_4)$.

3.2. Calculation section

It has been known that an aluminum atom or cation can interact with an ethene molecule to form a π-bonded complex. Alikhani et al. found that Al–C_2H_4 is a π-bonded complex with C_{2v} symmetry and $^2B_2$ ground state [19]. Krylov and Cristian also investigated the $^2B_2$ ground state and 11 lowest vertical excited states of the Al–C_2H_4 π-bonded complex with CCSD method [20]. Bowers and co-workers determined Al^+–C_2H_4 to be a C_{2v} symmetry structure with the Al^+ bonded side-on to C_2H_4 [24]. In this work, we calculated various structures of $Al^+(C_2H_4)_n$ (n = 1–3) clusters in order to understand the interaction of Al^+ ion with ethene molecules. The optimized structures of $Al^+(C_2H_4)_n$ (n = 1–3) clusters are shown in Fig. 3.

3.2.1. $Al^+(C_2H_4)$

We found three stable isomers for $Al^+(C_2H_4)$ cluster (Fig. 3). Isomer 1A is the most stable structure for $Al^+(C_2H_4)$. It has C_{2v} symmetry with $^1A_1$ ground electronic state. In isomer 1A, the Al^+ ion

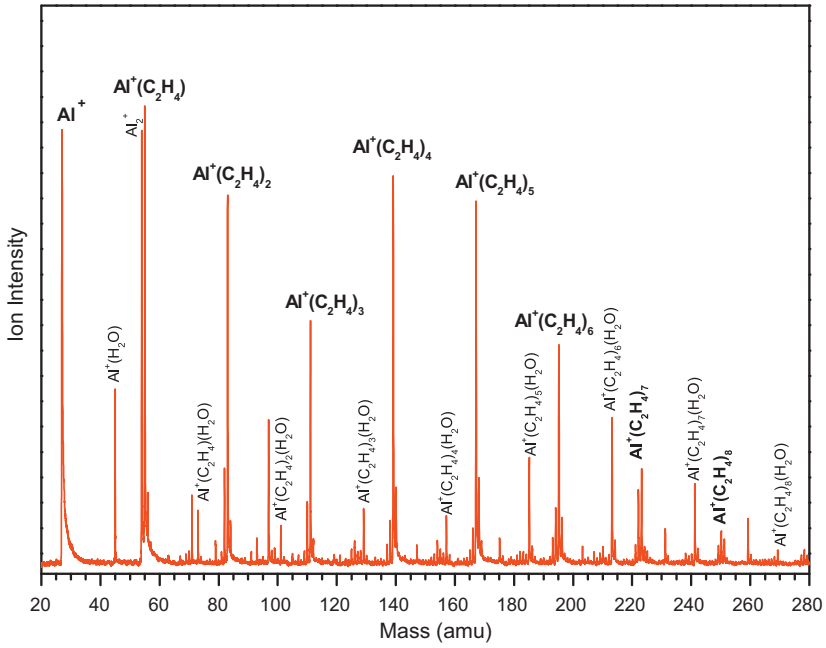

Fig. 1. Mass spectrum of $Al^+(C_2H_4)_n$ clusters.

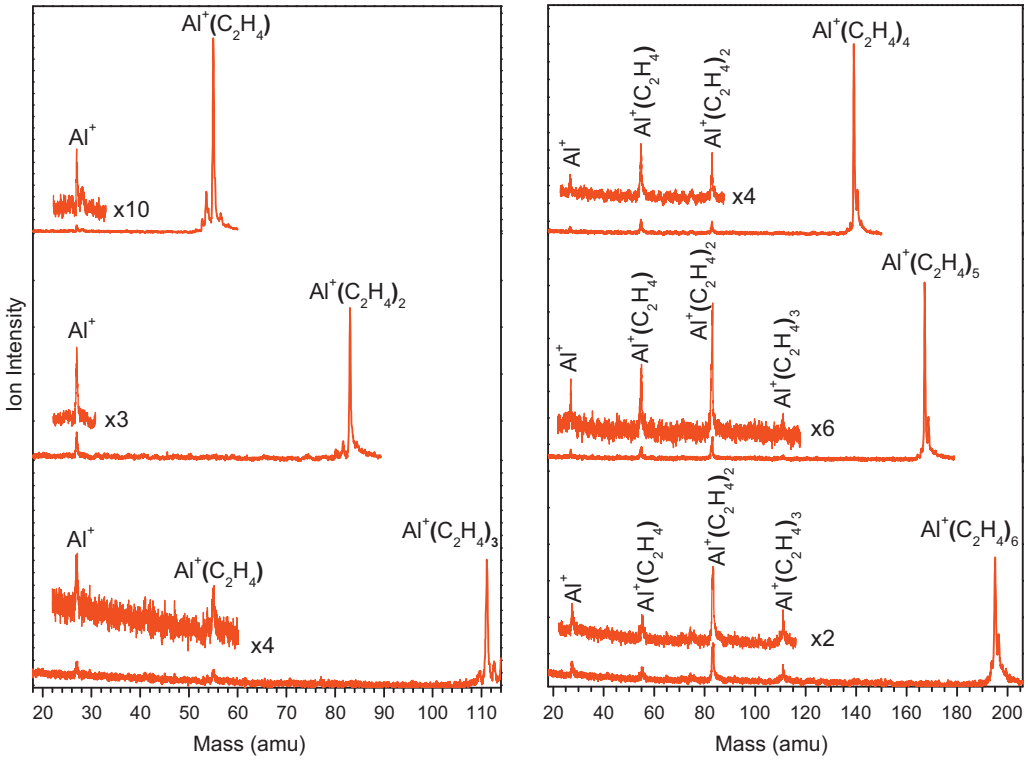

Fig. 2. Photodissociation mass spectra of $Al^+(C_2H_4)_n$ (n = 1–6) clusters at 266 nm.

attaches to the slightly disturbed ethene molecule. According to the MP2 calculation, isomer 1A has a T-shaped [25] equilibrium configuration with the dihedral angle ∠HCCH of 175°. The T-shaped structure here is defined as that Al^+ ion interacts with ethene in the perpendicular direction of the ethene molecular plane and the interaction between them is weak and the ethene molecule is only disturbed slightly. The C=C bond of isomer 1A is 1.35 Å, elongated by only 0.01 Å in comparison with that of free ethene molecule from experiment measurement [2] and the same theoretical calculation (1.34 Å) level. The Al–C distance is about 2.92 Å, considerably larger than the Al–C distance of 1.96 Å in trimethylaluminum in the gas phase [26], indicating that no Al–C covalent bond is formed in isomer 1A. Our calculations of isomer 1A are in agreement with those conducted by Kemper et al. [24]. The second isomer (1B) is a C_s structure in $^1A'$ electronic state. Isomer 1B is less stable than isomer 1A by about 0.75 eV. The most interesting thing is that isomer 1B is an inserted $[H–Al–CH=CH_2]^+$ species with the Al^+ ion inserted into the C–H bond of the ethene molecule. The Al–C and Al–H distances

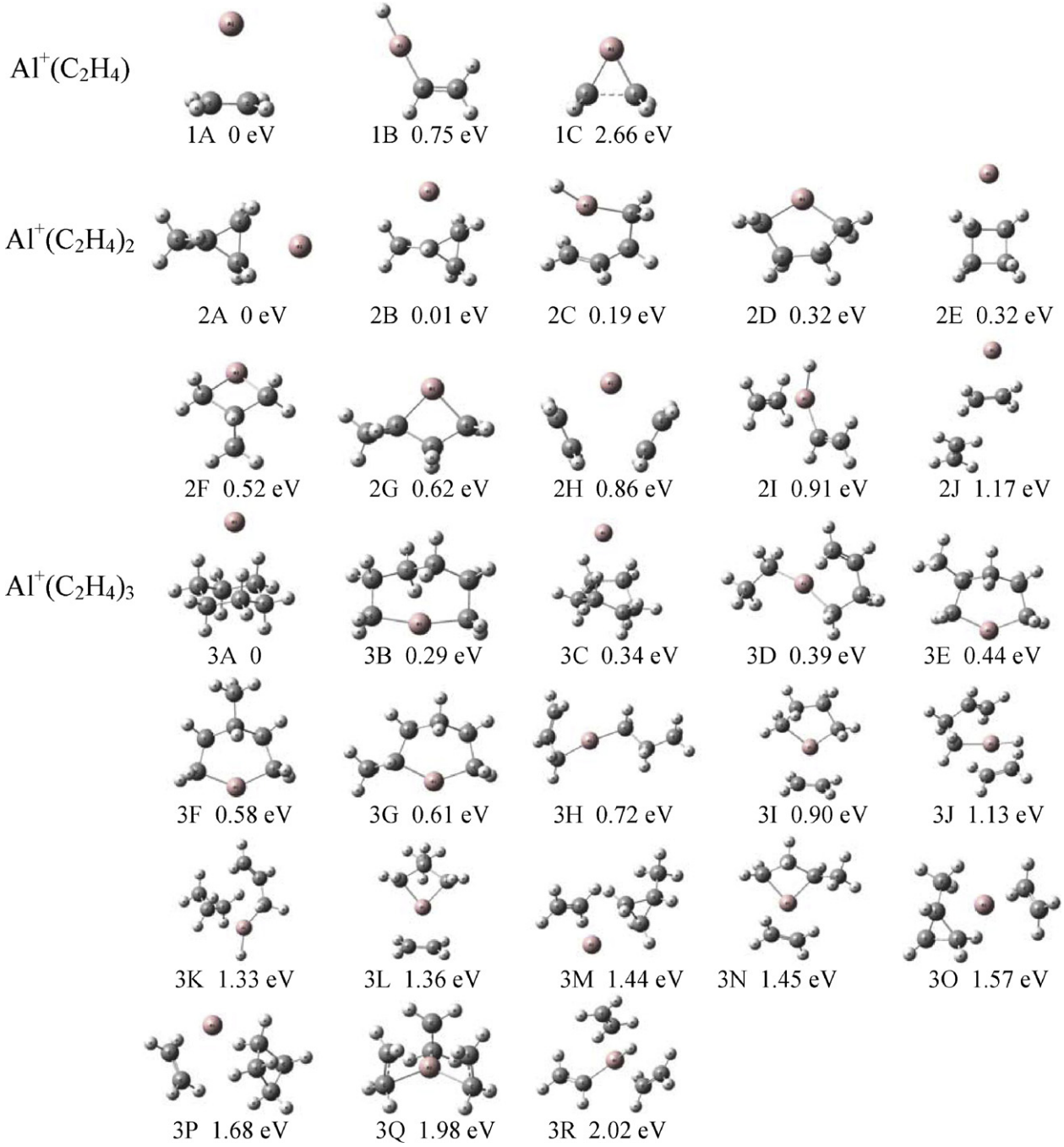

Fig. 3. Optimized structures of $Al^+(C_2H_4)_n$ (n = 1–3) clusters and their relative energies.

are 1.89 and 1.55 Å respectively. The calculations (Fig. 4) show that the energy barrier from isomer 1A to isomer 1B is about 3.61 eV, indicating that it is difficult to form isomer 1B. The third isomer (1C) of $Al^+(C_2H_4)$ has C_{2v} symmetry with $^1A_1$ electronic state. It is 2.66 eV higher than isomer 1A in energy. The two Al–C bonds in isomer 1C are both 1.89 Å. The C–C bond (1.76 Å) is longer than conventional C–C single bond (1.54 Å), indicating the C=C bond of the ethene molecule is broken due to the interaction with Al^+ ion.

In our experiment, the dissociation of $Al^+(C_2H_4)$ produces Al^+ fragment ion by loss of an ethene molecule. Thus, the existence of isomer 1B and 1C in our experiments can be ruled out. Isomer 1A is the most probable isomer detected in our experiments. The bond dissociation energy (BDE) of isomer 1A is calculated to be 0.49 eV, which is defined as $BDE = -(E_{Al^+(C2H4)} - E_{Al^+} - E_{C2H4})$. It is close to the value (0.59 eV) obtained by Schwarz and co-workers using *ab initio* methods [14] and is 0.17 eV lower than the experiment value of 0.66 eV measured by Bowers and co-workers [24]. Although the BDE of $Al^+(C_2H_4)$ (1A) is much lower than the photon energies of 1064, 532 and 355 nm, interestingly, no fragment of $Al^+(C_2H_4)$ was detected in the photodissociation experiments at these wavelengths. This can probably be explained by the low absorption cross-section at these wavelengths. As it has been shown by atomic spectral data, the first electronic excited state of Al^+ is 4.64 eV higher than its ground state [27]. It is expected that the first electronic excited state of $Al^+(C_2H_4)$ is similar to that of Al^+ since ethene can be consider as an unpolarized solvent molecule with little effect on the electronic state of Al^+ ion. In addition, ethene also has very high excited electronic state since it is a closed-shell molecule. Therefore, the $Al^+(C_2H_4)$ cluster probably does not absorb 1064, 532, and 355 nm photons. $Al^+(C_2H_4)$ is able to be dissociated at

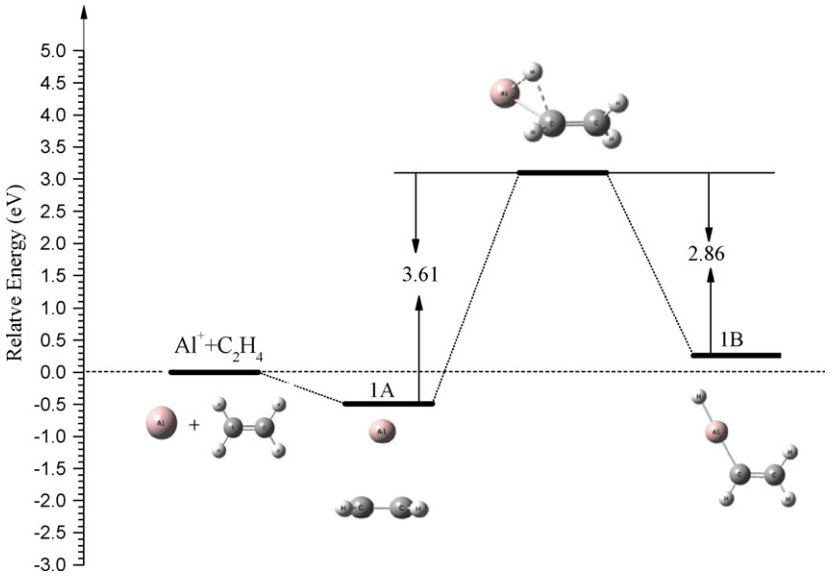

Fig. 4. The energy profile of isomer 1A, 1B and their transition state for $Al^+(C_2H_4)$ cluster.

266 nm because the photon energy of 266 nm is very close to the transition energy from the ground state of Al^+ ion to its first excited state.

3.2.2. $Al^+(C_2H_4)_2$

From relative energies in Fig. 3, we can see that isomer 2A and 2B are the most stable structures of $Al^+(C_2H_4)_2$. They are nearly degenerate in energy with isomer 2B higher than isomer 2A by only 0.01 eV. In isomers 2A and 2B, the two ethene molecules form a methyl cyclopropane which has weak interaction with the Al^+ ion. Isomer 2C is calculated to be 0.19 eV higher in energy than isomer 2A. It is an inserted structure with two ethene molecules bound together and the Al^+ ion inserted into one C–H bond, in which one of the two C=C bonds has become a C–C single bond. Isomer 2D is a non-planar five-member ring containing two Al–C σ-bonds, similar to the neutral aluminocyclopentane found by Chenier and co-workers using electron spin resonance at 77 K [13]. The Al–C bond length of isomer 2D is ~1.93 Å, which is also similar to the Al–C bond of trimethylaluminum (~1.96 Å) in the gas phase [26]. In isomer 2E, the two ethene molecules form a cyclobutane and the Al^+ ion interacts with the cyclobutane through one edge of the cyclobutane ring. Isomer 2E is 0.32 eV higher in energy than the most stable isomer of $Al^+(C_2H_4)_2$. In isomer 2F and isomer 2G, the Al^+ and three C atoms form a aluminocyclobutane and a methyl attaches to one of the C atoms of the aluminocyclobutane, locating at the para- or ortho-positions of the Al^+. Isomer 2H is a structure with two intact ethene molecules adsorbed by the Al^+ ion to form a weakly bound five-member ring. The initial structures that Al^+ ion binds to the C=C bonds of two ethene molecules in a π fashion with double bond parallel or perpendicular to each other were also considered, but they were optimized to isomer 2H. In isomer 2D and 2H, the two ethene molecules attach to the same side of Al^+ ion, owing to steric constraints imposed by electrons of the outmost 3s orbital of Al^+ ion. A similar effect happened in $Mg^+(ligands)_n$ and $Si^+(CO_2)_n$ clusters was also observed by other groups [28–33]. Isomer 2I is an inserted structure, in which the Al^+ ion inserts into one ethene molecule and the other ethene molecule is bound to the Al^+ ion of the $[H–Al–CH=CH_2]^+$ subunit. In isomer 2J, the Al^+ ion interacts with the first ethene molecule, and this ethene molecule interacts with the other ethene molecule.

Although the ten isomers of $Al^+(C_2H_4)_2$ mentioned above are all stable, which of them were produced in our experiments? Fig. 5 depicts the energy profile of the reactants (Al^+ and two ethene molecules), eight isomers of $Al^+(C_2H_4)_2$ and their transition states. It shows that there might be three possible reaction pathways for the formation of $Al^+(C_2H_4)_2$ isomers. Pathway (1): $Al^+(C_2H_4) + C_2H_4 \rightarrow 2H \rightarrow 2D$; Pathway (2): $Al^+(C_2H_4) + C_2H_4 \rightarrow 2J \rightarrow 2E$; Pathway (3): $Al^+(C_2H_4) + C_2H_4 \rightarrow 2H \rightarrow 2I \rightarrow 2C \rightarrow 2B \rightarrow 2G$. Isomer 2J is less stable than isomer 2H by 0.31 eV, which means the formation of isomer 2J is less possible. In addition, the energy barrier from isomer 2J to isomer 2E is quite large (1.36 eV), higher than the energy barrier of 0.15 eV from isomer 2H to 2D. That means the formation of isomer 2E is not possible. The energy barrier from isomer 2H to 2D is only 0.15 eV while that from isomer 2H to 2I is about 2.61 eV, which is much higher. Thus, Pathway (3) is also prohibited. Moreover, isomer 2D is more stable than isomer 2I by 0.59 eV. Overall, we found that Pathway (1), the pathway for the formation of isomer 2D, is the most probable pathway. Although isomer 2A, 2B, and 2C are lower in energy than isomer 2D, the energy barriers for their formation are much higher as can be seen in Pathway (3). The existence of isomer 2A, 2B, and 2C can be excluded from the experiment. Therefore, isomer 2D probably is the species generated in our source. This is consistent with the experimental results that two ethene molecules are eliminated for dissociation of $Al^+(C_2H_4)_2$ cluster.

3.2.3. $Al^+(C_2H_4)_3$

In Fig. 3, the lowest-energy structure is isomer 3A with the Al^+ ion interacting with a chair-like cyclohexane. The second stable structure is isomer 3B, a seven-member ring including an Al^+ ion and three ethene molecules coupled together, which is 0.29 eV higher in energy than 3A. The Al–C and C–C bond distances of isomer 3B are 1.94 Å, 1.55–1.56 Å. Isomer 3C has the Al^+ ion interacting with a boat-like cyclohexane. It is less stable than isomer 3A by 0.34 eV. Again, isomer 3A, 3B and 3C follows the binding pattern as same as isomers 2D and 2H of $Al^+(C_2H_4)_2$ where all ligands are located on the same side of the Al^+ ion. Isomer 3E, 3F and 3G are methyl aluminohexane in which there are two Al–C covalent bonds. Isomers 3D and 3H have chain structures with the Al^+ ion inserting into the carbon chains. Isomer 3I may originate from isomer 2D adsorbing one more ethene molecule. It is 0.9 eV higher in energy than isomer 3A. Isomer 3K is a structure with the Al^+ ion inserting into one C–H bond of propylene and adsorbing a cyclopropane. Isomer 3J, 3L, 3M, 3N, 3O, 3P, 3Q and 3R may evolve

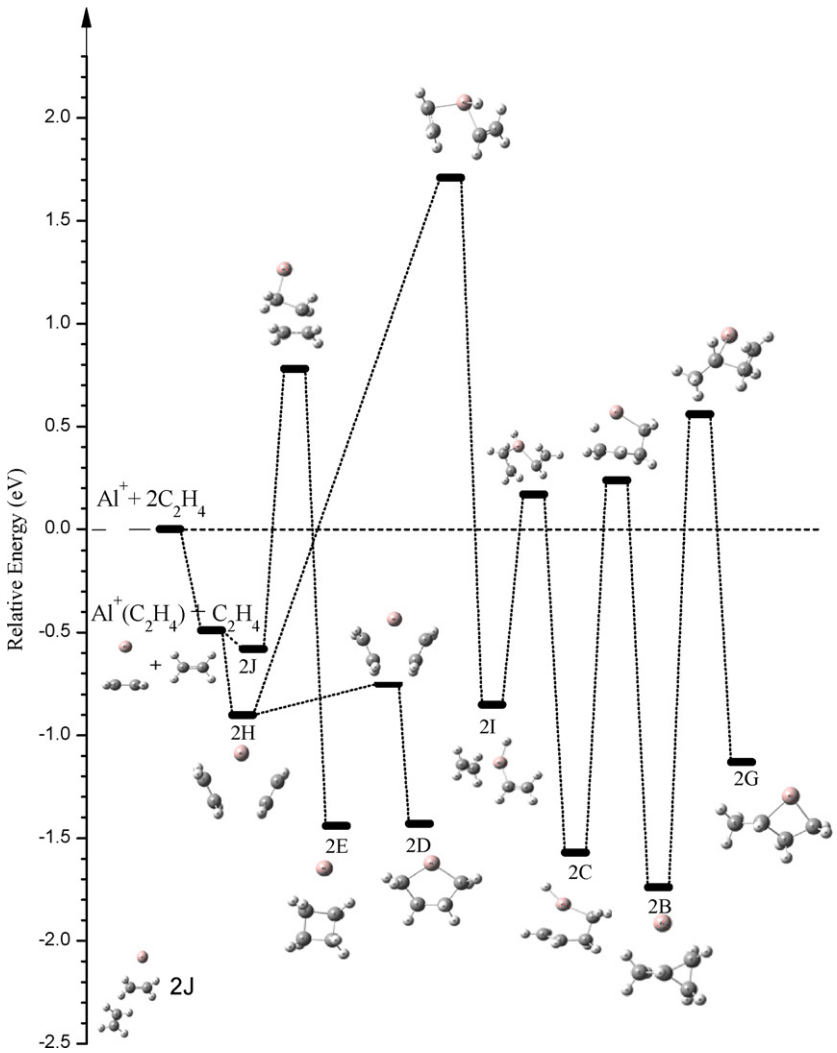

Fig. 5. The energy profile of eight isomers and their transition states for $Al^+(C_2H_4)_2$ cluster.

from isomer 2C, 2F, 2A, 2G, 2B, 2E, 2H and 2I, respectively, by adsorbing an additional ethene molecule. Since isomer 2C, 2F, 2A, 2G, 2B, 2E, 2H and 2I do not exist in our experiment, we suggest that isomers 3J and 3L–R of $Al^+(C_2H_4)_3$ probably do not exist in our experiment either. Based on the dissociation patterns of $Al^+(C_2H_4)_3$, i.e., two or three ethene molecules eliminated from $Al^+(C_2H_4)_3$ (Fig. 2), we suggest that isomers 3A, 3B and 3C are present in our experiments. However, the existence of isomer 3D–3I in the experiment cannot be ruled out.

Based on the isomers of $Al^+(C_2H_4)_{2-3}$ (2D, 3B) found in our experiments, we suggest that Al^+ and ethene molecules can form alumino-cycloalkane compounds. Regarding the Al-inserted structures $[H–Al–C_2H_3(C_2H_4)_n]^+$ (1B, 2C, 2I, 3J and 3R), our calculations show that the large barrier from isomer 1A to 1B (Fig. 4) prevents the formation of the inserted isomer 1B, the inserted $[H–Al–C_2H_3]^+$ core. Thus, the formation of inserted structures such as 1B, 2C, 2I, 3J and 3R in the experiment is not possible, although those isomers are found to be stationary points in the potential energy surfaces. The difficulties for the formation of inserted structures found by theoretical calculations are consistent with our experiments since the photodissociation mass spectra of $Al^+(C_2H_4)_n$ (n = 1–6) clusters provide no evidences for the existence of the $[H–Al–C_2H_3]^+(C_2H_4)_n$ (n = 1–5) isomers. The non-detection of inserted structure for $Al^+(C_2H_4)_n$ clusters is somewhat similar to the case of $Al^+(CH_4)_n$ that the inserted structures of $[H–Al–CH_3]^+(CH_4)_n$ (n = 1–5) are not detectable as shown by Bieske and co-workers using infrared photodissociation experiments and *ab initio* calculations [29].

It would be interesting to compare the $Al^+(C_2H_4)_n$ clusters with the $V^+(C_2H_4)_n$ clusters that we investigated before [34]. By comparing the mass spectra of $Al^+(C_2H_4)_n$ with that of $V^+(C_2H_4)_n$, we found that an Al^+ ion can form $Al^+(C_2H_4)_n$ clusters with more than eight ethene molecules while a V^+ ion can form $V^+(C_2H_4)_n$ clusters with no more than four ethene molecules [34]. Considering the photodissociation channels of $Al^+(C_2H_4)_n$ (n = 1–3) and $V^+(C_2H_4)_n$ (n = 1–3), we found that the dissociation channels of $Al^+(C_2H_4)_n$ (n = 2–3) are different from those of $V^+(C_2H_4)_n$ (n = 2–3), although the dissociation channels of $Al^+(C_2H_4)$ and $V^+(C_2H_4)$ are similar. For $V^+(C_2H_4)_2$, there are two dissociation channels: (1) $V^+(C_2H_4)_2 \rightarrow V^+(C_2H_4) + C_2H_4$, (2) $V^+(C_2H_4)_2 \rightarrow V^+ + 2C_2H_4$; while for $Al^+(C_2H_4)_2$, only one dissociation channel: $Al^+(C_2H_4)_2 \rightarrow Al^+ + 2C_2H_4$, was observed. For the dissociation of $V^+(C_2H_4)_3$, we observed three fragment ions, $V^+(C_2H_4)_2$, $V^+(C_2H_4)$ and V^+; while only two fragment ions, $Al^+(C_2H_4)$ and Al^+, were observed for the dissociation of $Al^+(C_2H_4)_3$. The facts indicate that the interaction between Al^+ and ethene is different from that between V^+ and ethene. As is shown by our calculations, in the structures of $Al^+(C_2H_4)_{2-3}$, the Al^+ can strongly interact with one or two C atoms to form Al–C σ-bonds and cause addition reaction between the ethene molecules.

Thus, the ethene molecules can form chain or ring structures. The chain and ring structures can be extended with addition of other ethene molecules. These are very similar to the uncatalyzed cationic cyclization reaction of $(C_2H_4)_{2-5}{}^+$ clusters reported by Lyktey et al. [35]. In $V^+(C_2H_4)_{2-3}$, the interaction between V^+ and the ethene molecules is quite weak, the interaction between the ethene molecules is also weak, and the C=C bond in the ethene molecules remain almost intact. The addition of more ethene molecules to $V^+(C_2H_4)_3$ is inhibited by the steric effects.

4. Conclusions

$Al^+(C_2H_4)_n$ clusters were produced in a supersonic molecular beam by laser vaporization and studied with laser photodissociation and *ab initio* calculations. For the dissociation of $Al^+(C_2H_4)_{2-5}$, the largest fragment ions were generated by loss of two ethene molecules. For the dissociation of $Al^+(C_2H_4)_6$, the largest fragment ion was generated by loss of three ethene molecules. The dissociation of $Al^+(C_2H_4)_n$ ($n = 1–6$) clusters can eliminate all ethene molecules to generate Al^+ fragment ion. Based on the photodissociation experiments and *ab initio* calculations, we would like to propose that: (1) Al–C σ-bonds can be formed in $Al^+(C_2H_4)_n$ ($n > 1$) clusters; (2) the strong interaction between Al^+ and ethene molecules can weaken the C=C bond significantly, thus, trigger addition reaction of ethene molecules to form chain or ring structures, such as aluminocyclopentane and aluminocycloheptane. In addition, formation of Al–C σ-bonds may explain why an Al^+ ion can combine with at least eight ethene molecules. However, these conclusions still need to be proved by further experimental and theoretical work.

Acknowledgements

This work was supported by the National Natural Science Foundation of China (NSFC, Grant No. 20933008). The theoretical calculations were conducted on the ScGrid and Deepcomp7000 of the Supercomputing Center, Computer Network Information Center of Chinese Academy of Sciences.

Appendix A. Supplementary data

Supplementary data associated with this article can be found, in the online version, at doi:10.1016/j.ijms.2011.08.026.

References

[1] J. Chen, T.H. Wong, P.D. Kleiber, K.H. Yang, J. Chem. Phys. 110 (1999) 11798.
[2] H. Zhou, H. Tamura, S. Takami, M. Kubo, R. Belosloudov, N. Zhanpeisov, A. Miyamoto, Appl. Surf. Sci. 158 (2000) 38.
[3] C. Emmeluth, B.L.J. Poad, C.D. Thompson, G. Weddle, E.J. Bieske, A.A. Buchachenko, T.A. Grinev, J. Klos, J. Chem. Phys. 127 (2007) 164310.
[4] D. Stockigt, J. Phys. Chem. A 102 (1998) 10493.
[5] C. Sishta, R.M. Hathorn, T.J. Marks, J. Am. Chem. Soc. 114 (1992) 1112.
[6] Y. Jiang, M. Hunger, W. Wang, J. Am. Chem. Soc. 128 (2006) 11679.
[7] J.Y. Yuan, X.C. Liao, H.M. Wang, G.Y. Yang, M.S. Tang, J. Phys. Chem. B 113 (2009) 1418.
[8] G.Y. Yang, Y.F. Ma, J. Xu, J. Am. Chem. Soc. 126 (2004) 10542.
[9] P.H. Kasai, D. McLeod, J. Am. Chem. Soc. 97 (1975) 5609.
[10] P.H. Kasai, J. Am. Chem. Soc. 104 (1982) 1165.
[11] S.A. Mitchell, B. Simard, D.M. Rayner, P.A. Hackett, J. Phys. Chem. 92 (1988) 1655.
[12] L. Manceron, L. Andrews, J. Phys. Chem. 93 (1989) 2964.
[13] J.H.B. Chenier, J.A. Howard, B. Mile, J. Am. Chem. Soc. 109 (1987) 4109.
[14] D. Stockigt, J. Schwarz, H. Schwarz, J. Phys. Chem. 100 (1996) 8786.
[15] J. Chen, T.H. Wong, Y.C. Cheng, K. Montgomery, P.D. Kleiber, J. Chem. Phys. 108 (1998) 2285.
[16] W.Y. Lu, R.G. Liu, T.H. Wong, J. Chen, P.D. Kleiber, J. Phys. Chem. A 106 (2002) 725.
[17] Y. Xie, B.F. Yates, Y. Yamaguchi, H.F. Schaefer, J. Am. Chem. Soc. 111 (1989) 6163.
[18] J. Fernandez Sanz, A. Marquez, J. Anguiano, J. Phys. Chem. 96 (1992) 6974.
[19] M.E. Alikhani, Y. Bouteiller, B. Silvi, J. Phys. Chem. 100 (1996) 16092.
[20] A.M.C. Cristian, A.I. Krylov, J. Chem. Phys. 118 (2003) 10912.
[21] Y.C. Zhao, Z.G. Zhang, J.Y. Yuan, H.G. Xu, W.J. Zheng, Chin. J. Chem. Phys. 22 (2009) 655.
[22] C. Moller, M.S. Plesset, Phys. Rev. 46 (1934) 618.
[23] M.J. Frisch, G.W. Trucks, H.B. Schlegel, G.E. Scuseria, M.A. Robb, J.R. Cheeseman, V.G. Zakrzewski, J.A. Montgomery Jr., R.E. Stratmann, J.C. Burant, S. Dapprich, J.M. Millam, A.D. Daniels, K.N. Kudin, M.C. Strain, O. Farkas, J. Tomasi, V. Barone, M. Cossi, R. Cammi, B. Mennucci, C. Pomelli, C. Adamo, S. Clifford, J. Ochterski, G.A. Petersson, P.Y. Ayala, Q. Cui, K. Morokuma, D.K. Malick, A.D. Rabuck, K. Raghavachari, J.B. Foresman, J. Cioslowski, J.V. Ortiz, A.G. Baboul, B.B. Stefanov, G. Liu, A. Liashenko, P. Piskorz, I. Komaromi, R. Gomperts, R.L. Martin, D.J. Fox, T. Keith, M.A. Al-Laham, C.Y. Peng, A. Nanayakkara, M. Challacombe, P.M.W. Gill, B. Johnson, W. Chen, M.W. Wong, C. Gonzalez, J.A. Pople, Gaussian 03, Gaussian, Inc., Wallingford, CT, 2004.
[24] P.R. Kemper, J. Bushnell, M.T. Bowers, G.I. Gellene, J. Phys. Chem. A 102 (1998) 8590.
[25] K.L. Stringer, M. Citir, R.B. Metz, J. Phys. Chem. A 108 (2004) 6996.
[26] A. Almenningen, S. Halvorsen, A. Haaland, Acta Chem. Scand. 25 (1971) 1937.
[27] J.E. Sansonetti, C. M.W., J. Phys. Chem. Ref. Data 34 (2005) 1571.
[28] Y. Mune, K. Ohashi, T. Iino, Y. Inokuchi, K. Judai, N. Nishi, H. Sekiya, Chem. Phys. Lett. 419 (2006) 201.
[29] B.L.J. Poad, C.D. Thompson, E.J. Bieske, Chem. Phys. 346 (2008) 176.
[30] K. Ohashi, K. Terabaru, Y. Inokuchi, Y. Mune, H. Machinaga, N. Nishi, H. Sekiya, Chem. Phys. Lett. 393 (2004) 264.
[31] R.S. Walters, N.R. Brinkmann, H.F. Schaefer, M.A. Duncan, J. Phys. Chem. A 107 (2003) 7396.
[32] G. Gregoire, N.R. Brinkmann, D. van Heijnsbergen, H.F. Schaefer, M.A. Duncan, J. Phys. Chem. A 107 (2003) 218.
[33] J.B. Jaeger, T.D. Jaeger, N.R. Brinkmann, H.F. Schaefer, M.A. Duncan, Can. J. Chem. 82 (2004) 934.
[34] J.Y. Yuan, Z.-G. Zhang, Y.C. Zhao, G.-L. Hou, H.-G. Xu, W.J. Zheng, J. Int. J. Mass. Spectrom. 295 (2010) 36.
[35] M.Y.M. Lyktey, T. Rycroft, J.F. Garvey, J. Phys. Chem. 100 (1996) 6427.